Chapter 2

Designing a Steady-State Tokamak

This chapter explores a simple model for designing steady-state tokamaks. In the next couple chapters, the model is first formalized for use in a systems code and then generalized to handle pulsed operation. These derivations highlight that the only difference between the two modes of operation is how they generate their auxiliary plasma current: LHCD for steady-state operation and inductive sources for when a reactor is purely pulsed.

Along the way, equations will be derived that get rather complicated. To remedy the situation, a distinction between dynamic~~floating~~ and static~~fixed~~ values is now given, which will allow splitting most equations into static~~fixed~~ and dynamic~~floating~~ parts. Dynamic~~Fixed~~ values – i.e. the tokamak's major radius (R_0) and magnet strength (B_0), as well as the plasma's current (I_P), temperature ($\overline{T}$), and density ($\overline{n}$) – are first-class variables in the model (see Table 3.1). Everything is derived to relate them. Static~~Fixed~~ values, on the other hand, can be treated as code inputs, which remain constant throughout a reactor solve. These most obviously include the various geometric and profile parameters introduced next section.

The overall structure of this chapter, then, is built around developing an equation for plasma current in a steady-state tokamak. It is shown that this value arises from balancing current in a reactor using both a plasma's own bootstrap current (I_{BS}), as well the tokamak's auxiliary driven current (I_{CD}). These relations necessitate geometric parameters and plasma profiles, which will be given shortly. Along the way, definitions will also be needed for the Greenwald density (N_G) and the fusion power (P_F). What is shown is that the current does not actually depend directly on the major radius (R_0) or magnet strength (B_0) of a tokamak – allowing these variables to be put off until next chapter.

2.1 Defining Plasma Parameters

As mentioned previously, the zero-dimensional model derived here can closely approximate solutions from higher-dimensional codes that might take many hours~~weeks~~ to run. The essence of boiling down three-dimensional behaviors to one dimensional profiles – and zero-dimensional averaged values – begins with defining the most important plasma parameters. These are the: current density (J), temperature (T), and density (n) of a plasma.

Solving this problem most generally usually involves decoupling the geometry of the plasma from the shaping of its nearly parabolic radial-profiles – both of which will be explained shortly.

2.1.1 Understanding Tokamak Geometry

The first thing people see when they look at a tokamak is its geometry – see Fig. 2-1. How big is it? Is it stretched out like a bicycle tire or compressed to the point of being nearly spherical? Would a slice across the major radius result in two cross-sections that were: circular, elliptic, or triangular?~~Is it stretched out like a tire or smooshed together like a bagel? If it were torn in two, would the exposed areas look like: circles, ovals, or triangles?~~

These questions lend themselves to the three important geometric variables – the inverse aspect ratio (ϵ), the elongation (κ), and the triangularity (δ). The inverse

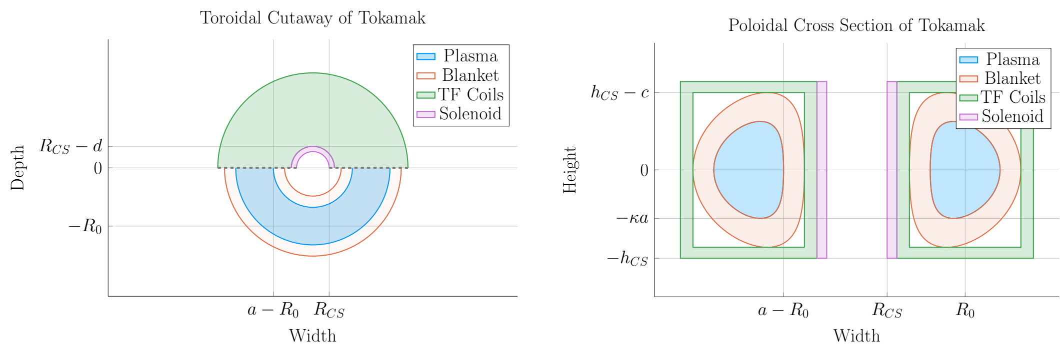

(a) Toroidal Cutaway (b) Poloidal Cross Section

Figure 2-1: Geometry of a Tokamak

This diagram is of a tokamak's toroidal (top) view and the poloidal cross section of a slice across the major axis. Included are the four components of a reactor: the plasma, it's metallic blanket, the toroidal field magnets surrounding them, and the central solenoid. These have thicknesses of a, b, c and d, respectively. R_{CS} is where the solenoid starts.

aspect ratio is a measure of how stretched out the device is, or formulaically:

$$a = \epsilon \cdot R_0 \tag{2.1}$$

This says that the minor radius (a), measured in meters, is related to the major radius of the machine (R_0) through ϵ. Or more tangibly, the minor radius is related to the two small cross-sections~~circles~~ that result from a slice across the major radius of the machine.~~come from tearing a bagel in two. Whereas the major radius is related to the overall circle of the bagel when viewing it from the top.~~

The remaining two geometric parameters – κ and δ – are related to the shape of the torn halves. As the name hints, elongation (κ) is a measure of how stretched out the tokamak is vertically – is the cross-section a circle or an oval? The triangularity (δ) is then how much the cross-sections point outward from the center of the device. All three's effects can be seen in Fig. 2-2. Their exact usage within describing flux surfaces is shown in Appendix E.

These geometric factors allow the volumetric and surface integrals governing fusion power and bootstrap current to be condensed to simple radial ones – see Eqs. (E.24)

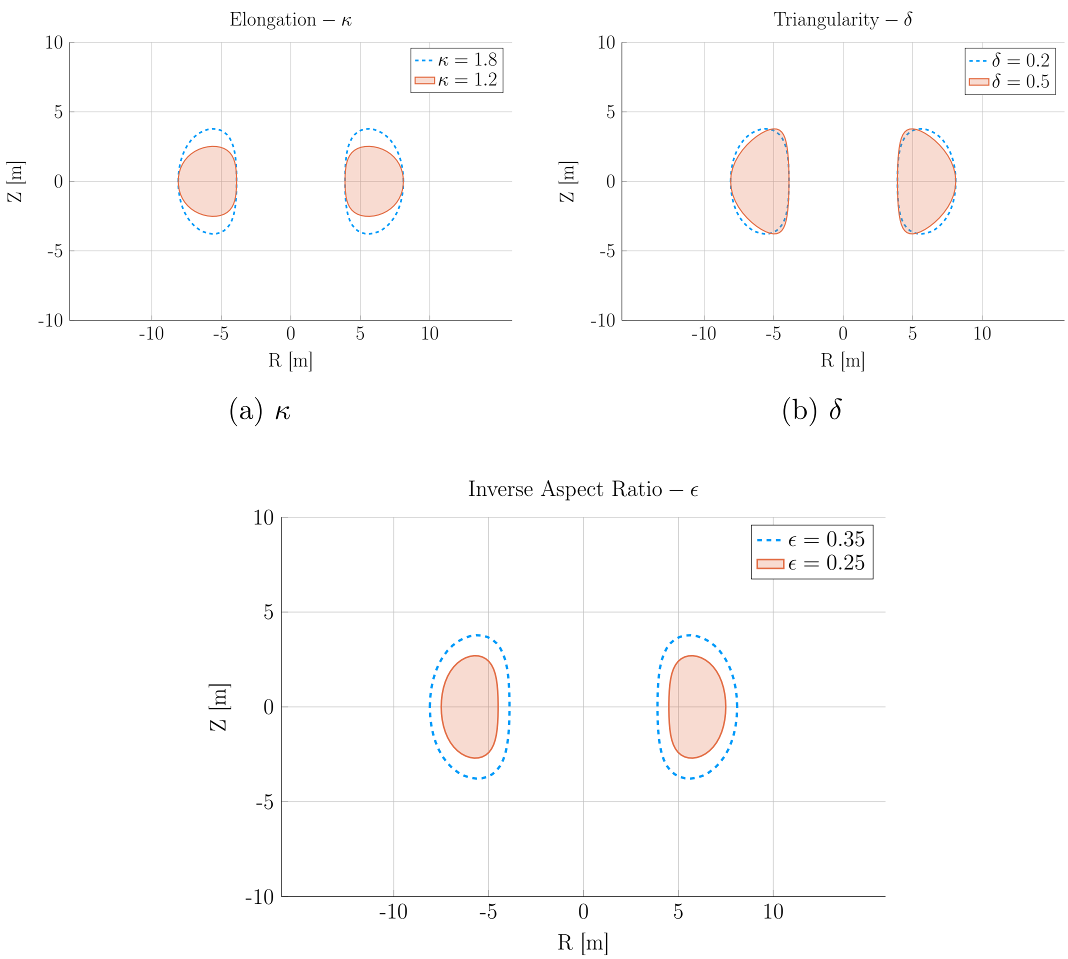

(a) κ (b) δ

(c) ϵ

Figure 2-2: Geometric Parameters

These three geometric parameters allow the toroidal cross-sections to scale radially, stretch vertically, and become more triangular – thus improving upon simple circular slices.

and (E.25). The only remaining step is to define the radial profiles for: the density, temperature, and current of a plasma.

2.1.2 Prescribing Plasma Profiles

The first step in defining radial profiles is realizing that all three quantities are essentially parabolas~~basically parabolas~~ – i.e. the temperature, density and current density, shown in Section 2.1.2, are peaked at some radius (usually the center) and then decay to zero somewhere before the walls of the tokamak enclosure.

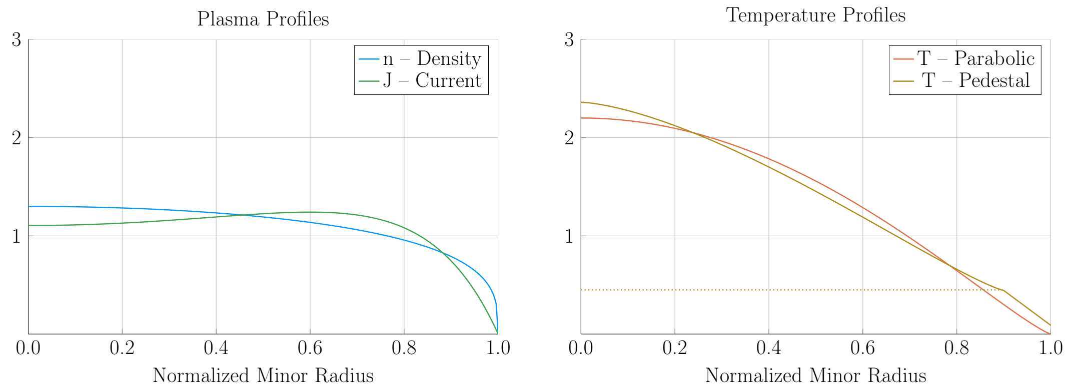

(a) Density and Current Profiles

(b) Temperature Profiles

Figure 2-3: Radial Plasma Profiles

The three most fundamental profiles~~properties~~ of a fusion plasma are its temperature, density, and current. These ~~profiles~~ allow the model to reduce from three dimensions to just half of one.

Although not self-consistent, these profiles do capture enough of the physics to approximate relevant phenomenon, such as transport and fusion power.[11]

The Density Profile

To begin, density has the simplest profile. This is because it is relatively flat, remaining near the average value – $\overline{n}$ – throughout the body of the plasma until quickly decaying to zero near the edge of the plasma.* For this reason, a parabolic profile with a very low peaking factor – ν_n – is well suited.

$$n(\rho) = \overline{n} \cdot (1 + \nu_n) \cdot (1 - \rho^2)^{\nu_n} \tag{2.2}$$

The reason $\overline{n}$ is referred to as the volume-averaged density is because using the volume integral – given by Eq. (E.24) – over the density profile results in that value

*Even in H-Mode plasmas where density profiles have a pedestal,[12] they usually have much less of a peak than temperatures[13] – especially so in a reactor setting.[14]

after dividing through by the volume ($\cancel{V}$):

$$\overline{n} = \frac{\int n(\mathbf{r})\, d\mathbf{r}}{\cancel{V}} \tag{2.3}$$

A final point to make is this parabolic profile allows for a short closed-form relation for the Greenwald density limit – substantially simplifying this fusion systems model.

The Temperature Profile

The use of a parabolic profile for the plasma temperature is slightly more dubious. This is because H-Mode plasmas are actually highly peaked at the center, decaying to a non-zero pedestal temperature near the edge before finally dropping sharply to zero. This model chooses to forego this pedestal representation for a simple parabolic one – although the pedestal approach is discussed in Appendix D. Analogous to the density, the profile treats $\overline{T}$ as the average value and ν_T as the peaking parameter.

$$T(\rho) = \overline{T} \cdot (1 + \nu_T) \cdot (1 - \rho^2)^{\nu_T} \tag{2.4}$$

The Current Density Profile

The plasma current density is the third profile and cannot safely be represented by a simple parabola. This is because having an adequate bootstrap current relies heavily on a profile being peaked off-axis – i.e. at some radius not at the center. This hollow profile can then be modeled with the commonly given plasma internal inductance (l_i). Concretely, the current's hollow profile is described by:

$$J(\rho) = \bar{J} \cdot \frac{\gamma^2 \cdot (1 - \rho^2) \cdot e^{\gamma \rho^2}}{e^{\gamma} - 1 - \gamma} \tag{2.5}$$

The intermediate γ quantity can then be numerically solved for from the plasma internal inductance using the following relations – with b_p representing the normalized poloidal magnetic field. These are derived in Appendix F.

$$l_i = \frac{4\kappa}{1+\kappa^2}\int_0^1 b_p^2\,\rho\,d\rho \tag{2.6}$$

$$b_p(\rho) = \frac{-e^{\gamma\rho^2}(\gamma\rho^2 - 1 - \gamma) - 1 - \gamma}{\rho\,(e^{\gamma} - 1 - \gamma)} \tag{2.7}$$

Combined, these three geometric parameters and profiles lay the foundation for this zero-dimensional fusion systems model.

2.2 Solving the Steady Current

As suggested, one of the most important equations in a fusion reactor is current balance. In steady-state operation, all of a plasma's current (I_P) must come from a combination of its own bootstrap current (I_{BS}), as well as auxiliary current drive (I_{CD}). This can be represented mathematically as:

$$\boxed{I_P = I_{BS} + I_{CD}} \tag{2.8}$$

The goal is then to write equations for bootstrap current and driven current. This will make heavy use of the Greenwald density limit. The steady current will then be~~Without spoiling too much, the steady current is~~ shown to be only a function of temperature! In other words, this current is independent of a tokamak's geometry and magnet strength. As will be pointed out then, though, a subtlety arises that will bring the two back into the picture – self-consistency in the current drive efficiency (η_{CD}).

2.2.1 Enforcing the Greenwald Density Limit

The Greenwald density limit is a density limit that applies to all tokamaks~~ubiquitous in the field of fusion energy.~~ It sets a hard limit on the density and how it scales with current and reactor size. Although currently lacking a true first-principles theoretical explanation, it does have a real meaning within the design context. Operate at too low a density and run the risk of never entering H-Mode. Run the density too high, and cause the tokamak's plasma to disrupt.~~disrupt catastrophically!~~ These conclusions can be seen in Fig. 2-4.

As no theoretical backing exists, the Greenwald density limit can simply be written (with citation) as:[15]

$$\hat{n} = N_G \cdot \left(\frac{I_P}{\pi a^2} \right) \tag{2.9}$$

Here, $\hat{n}$ has units of $10^{20}\ \frac{\text{particles}}{\text{m}^3}$, N_G is the Greenwald density fraction, and I_P is again the plasma current (measured in mega-amps). ~~and π has its usual meaning(3.141592653...).~~ The final variable is then the minor radius – a – which was previously defined through:

$$a = \epsilon \cdot R_0 \tag{2.1}$$

The next step is transforming the *line-averaged* density ($\hat{n}$) into the *volume-averaged* version ($\overline{n}$) used in this model. Harnessing the simplicity of the density's parabolic profile allows this relation to be written in a closed form as:

$$\hat{n} = \frac{\sqrt{\pi}}{2} \cdot \left(\frac{\Gamma\left(\nu_n + 2\right)}{\Gamma\left(\nu_n + \frac{3}{2}\right)} \right) \cdot \overline{n} \tag{2.10}$$

Where $\Gamma(\cdots)$ represents the gamma function: the non-integer analogue of the factorial function.

Combining these pieces allows the volume-averaged density to be written in standardized units ~~(i.e. the ones we use)~~ as:

$$\boxed{\overline{n} = K_n \cdot \left(\frac{I_P}{R_0^2} \right)} \tag{2.11}$$

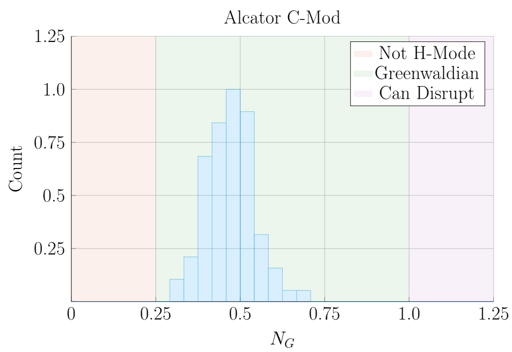

(a) C-Mod

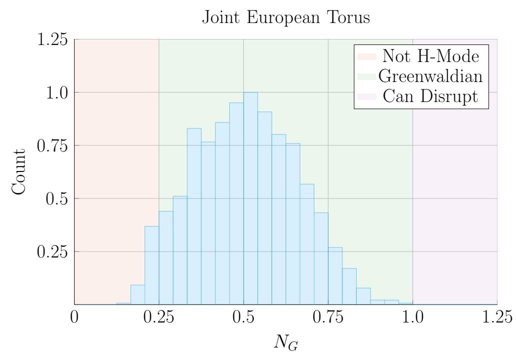

(b) JET

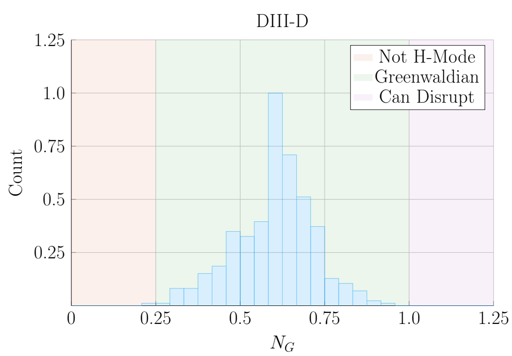

(c) DIII-D

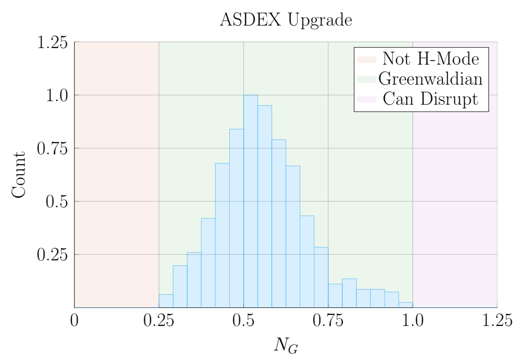

(d) ASDEX

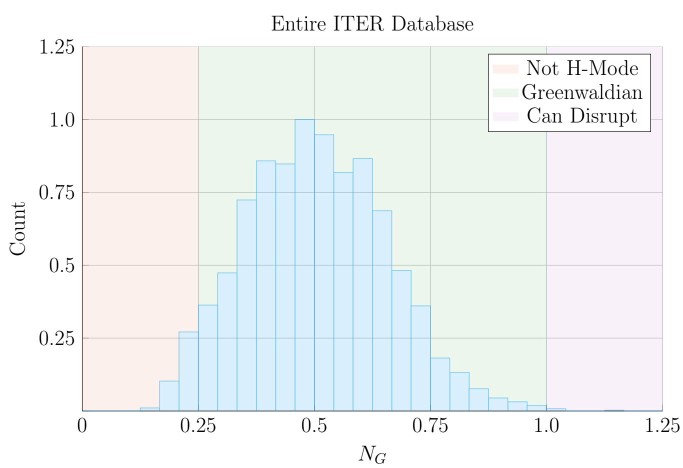

(e) All Tokamak Shots

Figure 2-4: Greenwald Density Limit

The Greenwald Density Limit is a robust metric of what densities an H-Mode plasma can attain. Although empirical in nature, it accurately predicts when a tokamak will undergo degraded plasma transport.[15]~~it is an indicator for good transport regimes.~~

$$K_n = \frac{2N_G}{\epsilon^2\,\pi^{3/2}} \cdot \left(\frac{\Gamma\left(\nu_n + \frac{3}{2}\right)}{\Gamma\left(\nu_n + 2\right)} \right) \tag{2.12}$$

The format of the previous equation pair will be used throughout the remainder of the paper. The top equation relates dynamic~~floating~~ variables (i.e. $\overline{n}$, I_P, and R_0), while the static~~fixed~~-value coefficient (K_n) lumps together static~~fixed~~ quantities, such as: N_G, ϵ, 2, π, and ν_n.

2.2.2 Declaring the Bootstrap Current

The first term to define in current balance, Eq. (2.8), is the bootstrap current. This bootstrap current is a mechanism of tokamak plasmas that helps supply some of the current needed to keep a plasma in equilibrium~~stable~~. Its underlying behavior stems from particles stuck in banana-shaped orbits on the outer edges of the device propelling the majority species along their helical trajectories around the tokamak. ~~From a hand-waving perspective, it involves particles stuck in banana-shaped orbits on the outer edges of a tokamak behaving like racing-game style speed boosts that accelerate charged particles along their hooped-shaped race tracks.~~

Utilizing the surface integral from Eq. (E.25), the bootstrap current (I_{BS}) can be written in terms of the temperature and density profiles: ~~To get an equation for bootstrap current, we must first introduce the surface integral – made possible from our previous choice of geometric parameters:~~

~~Here, Q is an arbitrary function of the normalized radius (ρ) and g is a geometric factor (of order 1):~~

~~This allows the bootstrap current (I_{BS}) to be written in terms of the temperature and density profiles:~~

$$I_{BS} = 2\pi a^2 \kappa g \int_0^1 J_{BS}\,\rho\,d\rho \tag{2.13}$$

$$\begin{aligned} J_{BS} &= f\left(n, T, \frac{dn}{d\rho}, \frac{dT}{d\rho}\right) \\ &\equiv -4.85 \cdot n \cdot T \cdot \frac{R_0 \sqrt{\epsilon\, \rho}}{{}^{d\psi}/_{d\rho}} \cdot \left(\frac{1}{n}\frac{dn}{d\rho} + 0.54\, \frac{1}{T}\frac{dT}{d\rho}\right) \end{aligned} \tag{2.14}$$

The second definition for the bootstrap current density – J_{BS} – comes from using well known theoretical results plus several simplifying assumptions, including the large aspect limit. The value of ${}^{d\psi}/_{d\rho}$ is given in Appendix F.

~~For a more formal look into this J_{BS} function, check the appendix section on pedestal temperatures. The point to make now is that it depends on the the profiles' derivatives, leading to one major discrepancy in the model.~~

As shown later in the results, bootstrap fractions are often under-predicted by this model. This is due to parabolic profiles (i.e. for temperature) having much less steep declines near the edge (i.e. in their derivatives) than characteristic H-Mode profiles with pedestals. This implies that the area most positively impacted by a pedestal profile for temperature would be the bootstrap current derivation. The instructions to do so are given in Appendix D.4.

~~Getting back on track – and without completeness – the bootstrap current can now be written in proportionality form as:~~

~~Recognizing that the last term is basically the inverse of the Greenwald density (see Eq. 2.11), allows the proportionality to be written in the following form. Note that this implies the bootstrap current is only a function of temperature!~~

~~In standardized units, this proportionality can be written as a concrete relation of the form:~~

Finally, summarizing the results of Appendix F, the bootstrap current is found to be only a function of temperature and static variables! In standardized units, it can be written as:

$$\boxed{I_{BS} = K_{BS} \cdot \overline{T}} \tag{2.15}$$

$$K_{BS} = 4.879 \cdot K_n \cdot \left(\frac{1+\kappa^2}{2} \right) \cdot \epsilon^{5/2} \cdot H_{BS} \tag{2.16}$$

$$H_{BS} = (1+\nu_n)(1+\nu_T)(\nu_n + 0.054\nu_T) \int_0^1 \frac{\rho^{5/2}\,(\,1-\rho^{\,2}\,)^{\,\nu_n+\nu_T-1}}{b_p}\, d\rho \tag{2.17}$$

Quickly noting, this H_{BS} term serves as the analogue of static~~fixed~~-value coefficients (e.g. K_{BS} and K_n) when they contain an integral. And b_p represents the poloidal magnet strength given by Eq. 2.7.

2.2.3 Deriving the Fusion Power

~~The next segue on our journey to solving for the steady current is deriving the fusion power (P_F), which appears in current drive. This requires a more first-principles approach than those used up until now. As such, a quick background is given to motivate the parameters it adds – i.e. the dilution factor (f_D) and the Bosch-Hale fusion reactivity (σv).~~

~~The natural place to start when talking about fusion is the binding-energy per nucleon plot (see Fig. N). As can be seen, the function reaches a maximum value around the element Iron (A=56). What this means at a basic level is: elements lighter than iron can *fuse* into a heavier one (i.e. hydrogens into helium), whereas heavier elements can *fission* into lighter ones (e.g. uranium into krypton and barium). This is what differentiates fission (uranium-fueled) reactors from fusion (hydrogen-fueled) ones. For fusion reactors, the most common reaction in a first-generation tokamak will be:~~

~~What this reaction describes is two isotopes of hydrogen – i.e. deuterium and tritium – fusing into a heavier element, helium, while simultaneously ejecting a neutron. The entire energy of the fusion reaction (E_F) is then divvied up 80-20 between the neutron and helium, respectively. Quantitatively, the helium (hereafter referred to as an alpha particle) receives 3.5 MeV.~~

~~The final point to make before returning to the fusion power derivation is the main difference between the two fusion products: helium (i.e. the alpha particle) and the~~

~~neutron. First, neutrons lack a charge – they are neutral. This means they cannot be confined with magnetic fields. As such, they simply move in straight lines until they collide with other particles. As the structure of a tokamak is mainly metal, the neutron is much more likely to collide there than the gaseous plasma, which is orders of magnitude less dense. Conversely, alpha particles are charged – when stripped of their electrons – and can therefore be kept within the plasma using magnets. What this means practically is that of the 17.6 MeV that comes from every fusion reaction, only 3.5 MeV remains inside the plasma (within the helium particle species).~~

The next segue on our journey to solving for the steady current is deriving the fusion power (P_F), which appears in current drive. A comprehensive introduction to this is given in Appendix C. Summarized, though, a formula for~~Returning to the problem at hand, the~~ fusion power from a D-T reaction – in megawatts – is given by the following volume integral:[?] ~~Jeff Freidberg's textbook through the following volume integral:~~

$$P_F = \int E_F \, n_D \, n_T \, \langle \sigma v \rangle \, d\mathbf{r} \tag{2.18}$$

$$E_F = 17.6 \text{ MeV} \tag{2.19}$$

The E_F quantity is the energy created from a deuterium-tritium fusion reaction. The n_D and n_T in this equation then represent the density of the deuterium and tritium ions, respectively. Assuming a 50-50 mix of the two, they can be related to the electron density – i.e. the one used in this model – through the dilution factor (f_D). This dilution factor represents the decrease in available fuel from part of the plasma actually being composed of non-hydrogen gasses:

$$n_D = n_T = f_D \cdot \left(\frac{n}{2} \right) \tag{2.20}$$

The fusion reactivity, $\langle \sigma v \rangle$, is then a nonlinear function of the temperature, T, which the model approximates using the Bosch-Hale tabulation (described in the appendix). As this tabulated value appears inside an integral, it seems important to point out that the temperature is now the most difficult dynamic~~floating~~ variable to handle –

over R_0, B_0, $\overline{n}$, and I_P. This will come into play when the model is formalized next chapter.

The next step in the derivation of fusion power is transforming the three-dimensional volume integral (see Eq. 2.18) into a zero-dimension averaged value. First, the volume analogue of the previously given surface-area integral is:

$$Q_V = 4\pi^2 R_0 a^2 \kappa g \int_0^1 Q(\rho)\rho \, d\rho \tag{2.21}$$

Where again, Q is an arbitrary function of ρ and g is a geometric factor approximately equal to one. The fusion power can now be rewritten as:

$$P_F = \pi^2 E_F f_D^2 R_0 a^2 \kappa g \int_0^1 n^2 \langle \sigma v \rangle \rho \, d\rho \tag{2.22}$$

In standardized units, this becomes:

$$\boxed{P_F = K_F \cdot \overline{n}^2 \cdot R_0^3 \cdot (\sigma v)} \tag{2.23}$$

$$K_F = 278.3 \cdot f_D^2 \cdot (\epsilon^2 \kappa g) \tag{2.24}$$

Where the standardized fusion reactivity is now,

$$(\sigma v) = 10^{21} \, (1+\nu_n)^2 \int_0^1 (1-\rho^2)^{2\nu_n} \langle \sigma v \rangle \, \rho \, d\rho \tag{2.25}$$

~~As mentioned before, this fusion power is divvied up 80-20 between the neutron and alpha particle. These relations will be used shortly. For now, they can be described mathematically as:~~ At this point, the current drive needed for steady-state can now be defined.

2.2.4 Using Current Drive

As may have been lost along the way, this chapter's~~the current~~ mission is to define a formula for steady current – from the current balance equation for steady-state tokamaks:

$$I_P = I_{BS} + I_{CD} \tag{2.8}$$

In standardized units, the equation for current drive is often given in the literature as:[16]

$$I_{CD} = \eta_{CD} \cdot \left(\frac{P_H}{\overline{n} R_0} \right) \tag{2.26}$$

Here, η_{CD} is the current drive efficiency with units $\left(\frac{\text{MA}}{\text{MW-m}^2}\right)$ and P_H is the heating power in megawatts driven by LHCD (and absorbed by the plasma).

Let it be known, though, that driving current in a plasma is hard! In fact, pulsed reactor designers (i.e. European fusion researchers) think it is so difficult, they may choose to forego it completely – focusing only on inductive sources that necessitate reactor fatigue and downtime.

A common current drive efficiency (η_{CD}) seen in many designs is 0.3 ± 0.1 in the standard units. It is however inherently a function of all the plasma parameters – with subtlety put off until the discussion of self-consistency. For now it assumed to have some constant/static~~fixed~~ value.

The remaining step in deriving an equation for driven current (I_{CD}) is a formula for the heating power (P_H). The way fusion systems models – like this one – handle the heating power is through the physics gain factor, Q. Sometimes referred to as big Q, this value represents how many times over the heating power (P_H) is amplified as it is transformed into fusion power (P_F):

$$P_H = \frac{P_F}{Q} \tag{2.27}$$

Now, utilizing the previously defined Greenwald density and fusion power:

$$\overline{n} = K_n \cdot \left(\frac{I_P}{R_0^2}\right) \tag{2.11}$$

$$P_F = K_F \cdot \overline{n}^2 \cdot R_0^3 \cdot (\sigma v) \tag{2.23}$$

The current from LHCD can be written as:

$$\boxed{I_{CD} = K_{CD} \cdot I_P \cdot (\sigma v)} \tag{2.28}$$

$$K_{CD} = (K_F K_n) \cdot \frac{\eta_{CD}}{Q} \tag{2.29}$$

As η_{CD} and Q appear within a static~~fixed~~ coefficient, it is implied that both remain constant throughout a solve. This subtlety is lifted when handling η_{CD} self-consistently, which will be discussed shortly. However, even in that context, it proves beneficial to still think of η_{CD} as a sequence of static~~fixed~~ variables – set by the model rather than the user.

2.2.5 Completing the Steady Current

The~~As hinted along the way, the~~ goal of this chapter~~section~~ has been to derive a simple formula for steady current (I_P). The problem started with current balance in a steady-state reactor:

$$I_P = I_{BS} + I_{CD} \tag{2.8}$$

Two equations were then found for the bootstrap (I_{BS}) and driven (I_{CD}) current:

$$I_{BS} = K_{BS} \cdot \overline{T} \tag{2.15}$$

$$I_{CD} = K_{CD} \cdot I_P \cdot (\sigma v) \tag{2.28}$$

Combining these three equations and solving for the total plasma current (I_P) – in mega-amps – yields:

$$\boxed{I_P = \frac{K_{BS}\,\overline{T}}{1 - K_{CD}(\sigma v)}} \tag{2.30}$$

This is the answer we have been seeking!

As mentioned before, this simple formula appears to only depend on temperature!* Apparently, the plasma should have the same current at some temperature (i.e. $\overline{T} =$ 15 keV), regardless of the size of the machine or the strength of its magnets. This has the important corollary that each temperature maps to only one current value. Further, each temperature would then map to a single magnet strength, capital cost, etc. (as shown next chapter).

As has become a mantra, though, the subtlety of this behavior lies in the self-consistency of the current-drive efficiency – η_{CD}.

2.3 Handling Current Drive Self-Consistently

Although a thorough description of the wave theory behind lower-hybrid current drive (LHCD) is well outside the scope of this text, it does motivate the solving of a tokamak's major radius (R_0) and field strength (B_0). It also shows how what was once a simple problem has now transformed into a rather complex one – a common occurrence with plasmas.

The logic behind finding a self-consistent current-drive efficiency is starting at some plausible value (i.e. $\eta_{CD} = 0.3$), solving for the steady current – i.e. $I_P = f(\overline{T})$ – and then somehow iteratively creeping towards a value deemed self-consistent. What this means is that in addition to the solver described in the last section, there needs to be a black-box function that solutions are sent~~piped~~ through to get better guesses at η_{CD}. The black-box function we use is a variation of the Ehst-Karney model.[17]

As mentioned, a self-consistent η_{CD} is found once a trip through the Ehst-Karney

*This dependence only on temperature refers to dynamic variables. The plasma current can still be highly volatile to many of the static variables, such as: ϵ, κ, N_G, f_D, ν_n, l_i, etc.

black-box results in the same η_{CD} as was sent~~piped~~ in – to some tolerable level of error. This consistency incorporates an explicit dependence on the tokamak configuration. Mathematically,

$$\tilde{\eta}_{CD} = f(R_0, B_0, \overline{n}, \overline{T}, I_P) \tag{2.31}$$

As such, to recalculate it after every solution of the steady current requires a value for both B_0 and R_0 – the targets of this model's primary and limiting~~secondary~~ constraints. These will be the highlight of the next chapter.

Appendix C

Discussing Fusion Power

In a tokamak reactor, the main source of output power is fusion. Therefore, this chapter goes over a quick background of fusion power and describes a method for how to calculate the reactivity term that appears inside it. The particular method used for this reactivity approximation was done by Bosch and Hale in 1992.[29]

C.1 Theoretical Background

The natural place to start when introducing fusion energy is the binding energy per nucleon curve shown in Fig. C-1. As can be seen, this function reaches a maximum value around the element Iron (A=56). What this means at a basic level is: elements lighter than iron can *fuse* into a heavier one (i.e. hydrogens into helium), whereas heavier elements can *fission* into lighter ones (e.g. uranium into krypton and barium). This is what differentiates fission (uranium-fueled) reactors from fusion (hydrogen-fueled) ones. For fusion reactors, the most common reaction in a first-generation tokamak will be:

$$^{2}H + {}^{3}H \rightarrow {}^{4}He + {}^{1}n + E_F \tag{C.1}$$

$$E_F = 17.6 \text{ MeV} \tag{C.2}$$

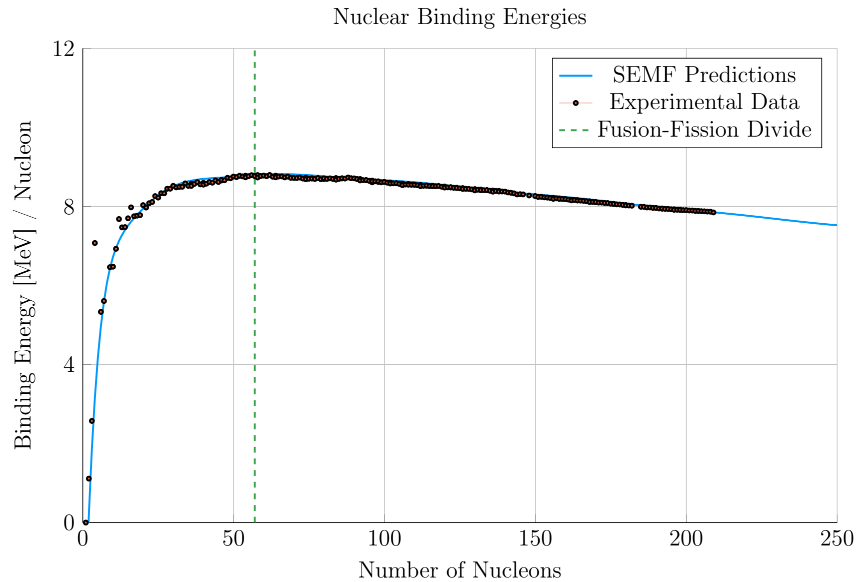

Figure C-1: Comparing Nuclear Fusion and Fission

The binding energy per nucleon is what differentiates nuclear fusion from fission. Nuclei heavier than Iron fission (e.g. Uranium), while light ones – such as Hydrogen – fuse.

What this reaction (shown in Fig. C-2) describes is two isotopes of hydrogen – i.e. deuterium and tritium – fusing into a heavier element, helium, while simultaneously ejecting a neutron. The entire energy of the fusion reaction (E_F) is then divvied up 80-20 between the neutron and helium, respectively. Quantitatively, the helium (often referred to as an alpha particle) receives 3.5 MeV.

$$P_n = 0.8 \cdot P_F \tag{C.3}$$

$$P_\alpha = 0.2 \cdot P_F \tag{C.4}$$

The final point to make is the main difference between the two fusion products: helium (i.e. the alpha particle) and the neutron. First, neutrons lack a charge – they are neutral. This means they cannot be confined with magnetic fields. As such, they simply move in straight lines until they collide with other particles. As the structure of a tokamak is mainly metal, the neutron is much more likely to collide there than the gaseous plasma, which is orders of magnitude less dense. Conversely, alpha particles

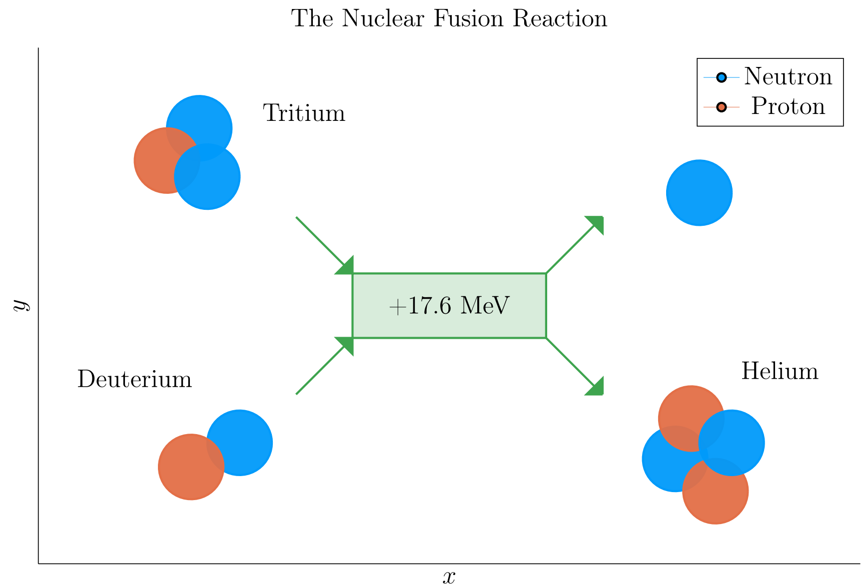

Figure C-2: The D-T Fusion Reaction

In a first generation tokamak reactor, the main source of energy will come from two hydrogen isotopes fusing into a helium particle – and ejecting a 14.1 MeV neutron.

are charged – when stripped of their electrons – and can therefore be kept within the plasma using magnets. What this means practically is that of the 17.6 MeV that comes from every fusion reaction, only 3.5 MeV remains inside the plasma (within the helium particle species).

C.2 Bosch-Hale Reactivity

The formula for fusion power used in this model makes use of a reactivity term – (σv):[4]

$$P_F = \int E_F \, n_D \, n_T \, \langle \sigma v \rangle \, d\mathbf{r} \tag{C.5}$$

Summarizing the work of Section 2.2.3, this fusion power volume integral can be reduced to a 0-D form – assuming the geometry prescribed by this model:

$$P_F = K_F \cdot (\,\overline{n}^2 \, R_0^3\,) \cdot (\sigma v) \quad [MW] \tag{C.6}$$

$$(\sigma v) = 10^{21}\,(1+\nu_n)^2 \int_0^1 (1-\rho^2)^{\,2\nu_n} \langle \sigma v \rangle \, \rho \, d\rho \tag{C.7}$$

$$K_F = 278.3\,(f_D^2\,\epsilon^2 \kappa\, g) \tag{C.8}$$

This reactivity term (or volumetric fusion reaction rate) can then be approximated by the Bosch-Hale parameterization, with coefficients given in Table C.1.[29,30]

$$\boxed{\langle \sigma v \rangle = C_1 \cdot \theta \cdot \exp(-3\xi) \cdot \sqrt{\frac{\xi}{m_\mu c^2 T^3}} \quad \left[{}^{\mathrm{m}^3}\!/\!{}_{\mathrm{s}}\right]} \tag{C.9}$$

$$\theta = T \cdot \left(1 - \frac{T(C_2 + T(C_4 + TC_6))}{1 + T(C_3 + T(C_5 + TC_7))}\right)^{-1} \tag{C.10}$$

$$\xi = \left(\frac{B_G^2}{4\theta}\right)^{1/3} \tag{C.11}$$

For D-T (Deuterium-Tritium) fuel within a standard fusion temperature regime (i.e. $T \in [10, 20]$ keV), this can be simplified to:[30]

$$\langle \sigma v \rangle_{\mathrm{DT}} = 1.1 \times 10^{-24} \cdot T^2 \quad \left[{}^{\mathrm{m}^3}\!/\!{}_{\mathrm{s}}\right] \tag{C.12}$$

In our model, each appearance of T is set to the radial profile defined earlier – as it appears inside an integral.

Example tabulations for this reactivity are given in Table C.2.[29–31]

Table C.1: Bosch-Hale parametrization coefficients for volumetric reaction rates

	^{2}H(d,n)^{3}He	^{2}H(d,p)^{3}H	^{3}H(d,n)^{4}He	^{3}He(d,p)^{4}He
B_G [keV$^{1/2}$]	31.3970	31.3970	34.3827	68.7508
$m_\mu c^2$ [keV]	937 814	937 814	1 124 656	1 124 572
C_1	5.43360×10^{-12}	5.65718×10^{-12}	1.17302×10^{-9}	5.51036×10^{-10}
C_2	5.85778×10^{-3}	3.41267×10^{-3}	1.51361×10^{-2}	6.41918×10^{-3}
C_3	7.68222×10^{-3}	1.99167×10^{-3}	7.51886×10^{-2}	-2.02896×10^{-3}
C_4	0.0	0.0	4.60643×10^{-3}	-1.91080×10^{-5}
C_5	-2.96400×10^{-6}	1.05060×10^{-5}	1.35000×10^{-2}	1.35776×10^{-4}
C_6	0.0	0.0	-1.06750×10^{-4}	0.0
C_7	0.0	0.0	1.36600×10^{-5}	0.0
Valid range (keV)	$0.2<T_i<100$	$0.2<T_i<100$	$0.2<T_i<100$	$0.5<T_i<190$

Table C.2: Tabulated Bosch-Hale reaction rates [m^3 s^{-1}]

T (keV)	^{2}H(d,n)^{3}He	^{2}H(d,p)^{3}H	^{3}H(d,n)^{4}He	^{3}He(d,p)^{4}He
1.0	9.933×10^{-29}	1.017×10^{-28}	6.857×10^{-27}	3.057×10^{-32}
1.5	8.284×10^{-28}	8.431×10^{-28}	6.923×10^{-26}	1.317×10^{-30}
2.0	3.110×10^{-27}	3.150×10^{-27}	2.977×10^{-25}	1.399×10^{-29}
3.0	1.602×10^{-26}	1.608×10^{-26}	1.867×10^{-24}	2.676×10^{-28}
4.0	4.447×10^{-26}	4.428×10^{-26}	5.974×10^{-24}	1.710×10^{-27}
5.0	9.128×10^{-26}	9.024×10^{-26}	1.366×10^{-23}	6.377×10^{-27}
8.0	3.457×10^{-25}	3.354×10^{-25}	6.222×10^{-23}	7.504×10^{-26}
10.0	6.023×10^{-25}	5.781×10^{-25}	1.136×10^{-22}	2.126×10^{-25}
12.0	9.175×10^{-25}	8.723×10^{-25}	1.747×10^{-22}	4.715×10^{-25}
15.0	1.481×10^{-24}	1.390×10^{-24}	2.740×10^{-22}	1.175×10^{-24}
20.0	2.603×10^{-24}	2.399×10^{-24}	4.330×10^{-22}	3.482×10^{-24}

Bibliography

[1] W Biel, M Beckers, R Kemp, R Wenninger, and H Zohm. Systems code studies on the optimization of design parameters for a pulsed DEMO tokamak reactor, 2016.

[2] C E Kessel, M S Tillack, F Najmabadi, F M Poli, K Ghantous, N Gorelenkov, X R Wang, D Navaei, H H Toudeshki, C Koehly, L El-Guebaly, J P Blanchard, C J Martin, L Mynsburge, P Humrickhouse, M E Rensink, T D Rognlien, M Yoda, S I Abdel-Khalik, M D Hageman, B H Mills, J D Rader, D L Sadowski, P B Snyder, H. St. John, A D Turnbull, L M Waganer, S Malang, and A F Rowcliffe. The ARIES advanced and conservative tokamak power plant study. *Fusion Science and Technology*, 67(1):1–21, 2015.

[3] GS Lee, J Kim, SM Hwang, Choong-Seock Chang, Hong-Young Chang, MH Cho, BH Choi, K Kim, KW Cho, S Cho, et al. The kstar project: An advanced steady state superconducting tokamak experiment. *Nuclear Fusion*, 40(3Y):575, 2000.

[4] Jeffrey P Freidberg. *Plasma Physics and Fusion Energy*, volume 1. 2007.

[5] B. N. Sorbom, J. Ball, T. R. Palmer, F. J. Mangiarotti, J. M. Sierchio, P. Bonoli, C. Kasten, D. A. Sutherland, H. S. Barnard, C. B. Haakonsen, J. Goh, C. Sung, and D. G. Whyte. ARC: A compact, high-field, fusion nuclear science facility and demonstration power plant with demountable magnets. *Fusion Engineering and Design*, 100:378–405, nov 2015.

[6] M Kovari, R Kemp, H Lux, P Knight, J Morris, and D J Ward. " PROCESS " : A systems code for fusion power plantsâĂŤPart 1: Physics. *Fusion Engineering and Design*, 89(12):3054–3069, 2014.

[7] Meszaros et al. Demo I Input File.

[8] H. Fountain. A dream of clean energy at a very high price. `https://www.nytimes.com/2017/03/27/science/fusion-power-plant-iter-france.html`, 2017. Accessed: 2018-12-6.

[9] J. Tirone. WorldâĂŹs biggest science experiment seeks more time and money. `https://www.bloomberg.com/news/articles/2016-06-15/world-s-biggest-science-experiment-seeks-more-time-and-money`, 2016. Accessed: 2018-12-6.

[10] David J. Griffiths. *Introduction to electrodynamics.*

[11] P J Knight and M D Kovari. A User Guide to the PROCESS Fusion Reactor Systems Code, 2016.

[12] D C Mcdonald, J G Cordey, K Thomsen, C Angioni, H Weisen, O J W F Kardaun, M Maslov, A Zabolotsky, C Fuchs, L Garzotti, C Giroud, B Kurzan, P Mantica, A G Peeters, and J Stober. Scaling of density peaking in H-mode plasmas based on a combined database of AUG and JET observations. *Nucl. Fusion*, 47:1326–1335, 2018.

[13] T Onjun, G Bateman, A H Kritz, and G Hammett. Models for the pedestal temperature at the edge of H-mode tokamak plasmas. *Physics of Plasmas*, 9(10), 2002.

[14] G Saibene, L D Horton, R Sartori, and A E Hubbard. Physics and scaling of the H-mode pedestal The influence of isotope mass, edge magnetic shear and input power on high density ELMy H modes in JET Physics and scaling of the H-mode pedestal. *Control. Fusion*, 42:15–35, 2000.

[15] Martin Greenwald. Density limits in toroidal plasmas, 2002.

[16] J Jacquinot,) Jet, S Putvinski,) Jct, G Bosia, Jct), A Fukuyama, U) Okayama, R Hemsworth, Cea Cadarache), S Konovalov, Rrc Kurchatov), W M Nevins, Llnl), F Perkins, K A Rasumova, Rrc-) Kurchatov, F Romanelli, Enea-) Frascati, K Tobita, Jaeri), K Ushigusa, J W Van, U Dam, V Texas), Rrc Vdovin, S Kurchatov), R Zweben, Erm Koch, Kms-) Brussels, J.-G Wégrowe, Cea-) Cadarache, V V Alikaev, B Beaumont, A Bécoulet, S Bern-Abei, Pppl), V P Bhatnagar, Ec Brussels), S Brémond, and M D Carter. Chapter 6: Plasma auxiliary heating and current drive. *ITER Physics Basis Editors Nucl. Fusion*, 39, 1999.

[17] D A Ehst and C F F Karney. Approximate formula for radiofrequency current drive efficiency with magnetic trapping, 1991.

[18] Ian H Hutchinson. Principles of plasma diagnostics. *Plasma Physics and Controlled Fusion*, 44(12):2603, 2002.

[19] Tobias Hartmann, Thomas Hamacher, Hon-Prof rer nat Hartmut Zohm, and Hon-Prof rer nat Sibylle Günter. Development of a Modular Systems Code to Analyse the Implications of Physics Assumptions on the Design of a Demonstration Fusion Power Plant.

[20] N A Uckan. ITER Physics Design Guidelines at High Aspect Ratio. pages 1–4, 2009.

[21] J P Freidberg, F J Mangiarotti, and J Minervini. Designing a tokamak fusion reactor - How does plasma physics fit in? *Physics of Plasmas*, 22(7):070901, 2015.

[22] B Labombard, E Marmar, J Irby, T Rognlien, and M Umansky. ADX: a high field, high power density, advanced divertor and RF tokamak Nuclear Fusion. Technical report, 2017.

[23] S P Hirshman and G H Neilson. External inductance of an axisymmetric plasma. *Physics of Fluids*, 29(3):790–793, 1986.

[24] P Libeyre, N Mitchell, D Bessette, Y Gribov, C Jong, and C Lyraud. Detailed design of the ITER central solenoid. *Fusion Engineering and Design*, 84:1188–1191, 2009.

[25] Jeff P Freidberg, Antoin Cerfon, and Jungpyo Lee. Tokamak elongation: how much is too much? I Theory. *arXiv.org*, pages 1–34, 2015.

[26] E. J. Doyle, W. A. Houlberg, Y. Kamada, V. Mukhovatov, T. H. Osborne, A. Polevoi, G Bateman, J. W. Connor, J. G. Cordey, T Fujita, X Garbet, T. S. Hahm, L. D. Horton, A. E. Hubbard, F Imbeaux, F Jenko, J. E. Kinsey, Y Kishimoto, J Li, T. C. Luce, Y Martin, M Ossipenko, V Parail, A Peeters, T. L. Rhodes, J. E. Rice, C. M. Roach, V Rozhansky, F Ryter, G Saibene, R Sartori, A. C.C. Sips, J. A. Snipes, M Sugihara, E. J. Synakowski, H Takenaga, T Takizuka, K Thomsen, M. R. Wade, and H. R. Wilson. Chapter 2: Plasma confinement and transport. *Nuclear Fusion*, 47(6):S18–S127, jun 2007.

[27] H Lux, R Kemp, E Fable, and R Wenninger. Radiation and confinement in 0-D fusion systems codes. Technical report.

[28] Louis Giannone, J Baldzuhn, R Burhenn, P Grigull, U Stroth, F Wagner, R Brakel, C Fuchs, HJ Hartfuss, K McCormick, et al. Physics of the density limit in the w7-as stellarator. *Plasma physics and controlled fusion*, 42(6):603, 2000.

[29] H Bosch and G M Hale. Improved formulas for fusion cross-sections and thermal reactivities. 611.

[30] Zachary S Hartwig and Yuri A Podpaly. Magnetic Fusion Energy Formulary. Technical report, 2014.

[31] Joseph D Huba. Nrl plasma formulary. Technical report, NAVAL RESEARCH LAB WASHINGTON DC PLASMA PHYSICS DIV, 2006.

[32] John Wesson and David J Campbell. *Tokamaks*, volume 149. Oxford University Press, 2011.

[33] C. E. Kessel. Bootstrap current in a tokamak. *Nuclear Fusion*, 34(9):1221–1238, 1994.